

NUCLEAR PHYSICS OVER THE YEARS: FROM THE HIGH-SPIN ERA TO RARE ISOTOPES

GAMMASPHERE EXPERIMENTS WITH ROBERT: EXAMPLES FROM A HERCULEAN EFFORT

WALTER REVIOL
ANL Physics Division

09/19/2025
UNC Conference Center
Chapel Hill

ACKNOWLEDGEMENT
GSFMA154/202/263 collaborations;
J. Davis, V. Tripathi, I. Wiedenhöver,
L. Sobotka



Some of today's themes

I. Angular momentum in nuclear fission and tests of the six fission modes



II. Tests of the simplex quantum number in odd-mass actinide nuclei and parity doublets; brief excursion into measuring atomic electric dipole moments



NB The nuclear physics data of this presentation are from experiments w/ Gammasphere and HERCULES



64 fast-plastic detectors

$4.1^\circ \leq \theta \leq 26.8^\circ$, $D_{\text{source/target}} = 23.2 \text{ cm}$

Segmentation determines fission axis (expt. I)

However, residue counting is prime application (experiments II)

AVERAGE SPINS OF PRIMARY FISSION FRAGMENTS

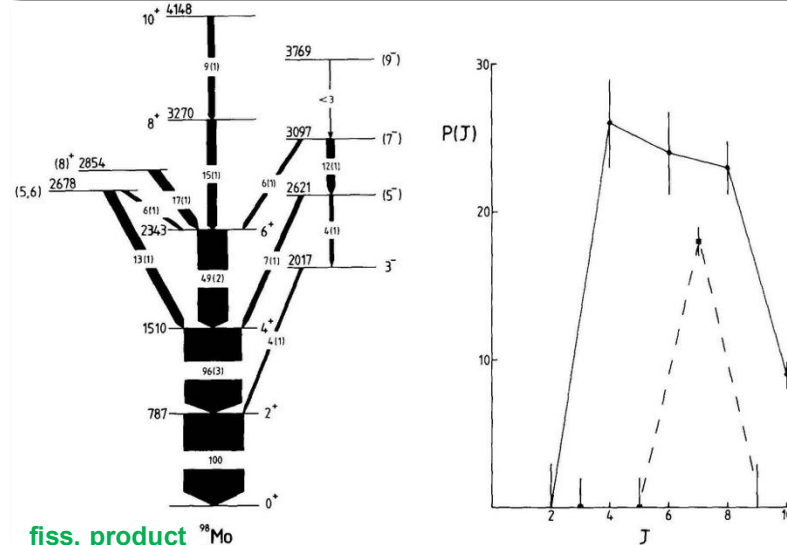
Y. ABDELRAHMAN, J.L. DURELL, W. GELLETLY, W.R. PHILLIPS
Department of Physics, University of Manchester, Manchester, M13 9PL, UK

I. AHMAD, R. HOLZMANN, R.V.F. JANSSENS, T.L. KHOO, W.C. MA
Argonne National Laboratory, Argonne, IL 60439, USA

and

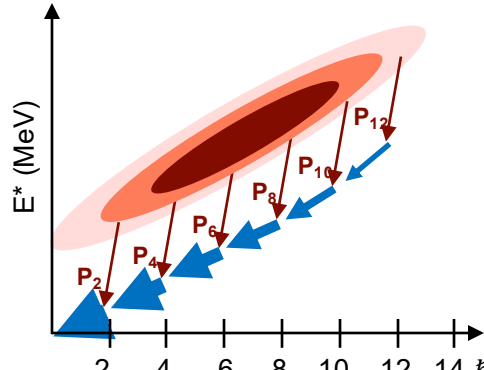
M.W. DRIGERT

University of Notre Dame, IN 46556, USA



$$E_{\text{lab}} = 120 \text{ MeV}$$

8 Compton-supp'd HPGe [I_γ (yrast)]
 14 BGO hexagonal crystals ($m_{i,\text{avg}}$)



Additional comments

Similar study done
 by Wilhelmy et al.
PRC 5, 2041 (1972);
 but with a ^{252}Cf SF
 source.

Source experiments
 are the workhorse
 for such studies;
 Robert did several
 of these too including
 the one 6 slides later.

Angular momentum generation in nuclear fission

566 | Nature | Vol 590 | 25 February 2021

<https://doi.org/10.1038/s41586-021-0330-4-w>

Received: 18 June 2020

Accepted: 9 December 2020

Published online: 24 February 2021



French lead collaboration
(IJC Lab Orsay)

J. N. Wilson¹ , D. Thisse¹, M. Lebois¹, N. Jovančević², D. Gjestvang², R. Canavan^{3,4}, M. Rudigier^{3,5}, D. Étasse⁶, R-B. Gerst⁷, L. Gaudefroy⁸, E. Adamska⁹, P. Adsley¹, A. Algora^{10,11}, M. Babo¹, K. Belvedere², J. Benito², G. Benzon¹², A. Blazhev¹³, A. Boso⁴, S. Bottom^{13,14}, M. Bunce⁴, R. Chakma¹, N. Cieplińska-Oryńczak¹⁰, S. Courtin¹⁶, M. L. Cortés¹⁷, P. Davies¹⁸, C. Delafosse¹, M. Fallot¹⁹, B. Fornal¹⁵, L. Fraisse¹², A. Gottardo²⁰, V. Guadilla¹⁹, G. Häfner¹⁷, K. Hauschild¹, M. Helme¹⁶, C. Henrich¹, I. Homm¹, F. Ibrahim¹, L. W. Iskra^{13,15}, P. Ivanov¹, S. Jazrawi^{13,4}, A. Kongul¹, P. Koseoglou^{2,21}, T. Kröll¹⁸, T. Kurtukian-Nieto²², L. Le Meur¹⁹, S. Leon^{13,14}, J. Ljungvall¹, A. Lopez-Martens¹, R. Lozeva¹, I. Matea¹, K. Miernik¹, J. Nemer¹, S. Oberstedt²³, W. Paulsen², M. Piessa⁹, Y. Popovitch¹, C. Porzio^{12,14,24}, L. Qi¹, D. Ralev²⁵, P. H. Regan^{3,4}, K. Rezynkina²⁶, V. Sánchez-Tembleque¹², S. Siem², C. Schmitt¹⁸, P.-A. Söderström^{2,27}, C. Sürder³, G. Tocabens¹, V. Vedia¹², D. Verney¹, N. War⁷, B. Wasilewska¹⁵, J. Wiederhold⁴, M. Yavahchova²⁶, F. Zeiser² & S. Zillani^{13,14}

Finding 1: spin sawtooth confirmed

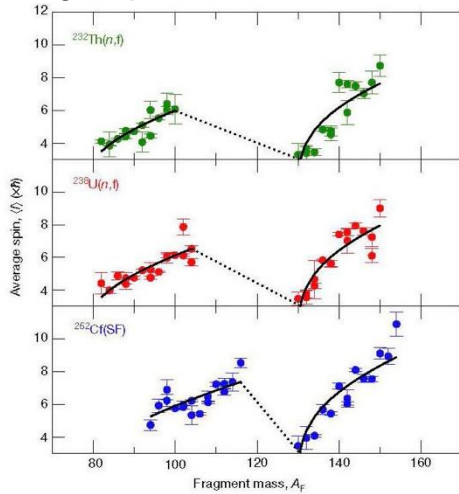


Fig. 1 | Dependence of average spin on fragment mass. Average spins extracted for even–even nuclei produced in fast-neutron-induced fission of ^{232}Th , ^{238}U and the spontaneous fission (SF) of ^{252}Cf are presented along with statistical uncertainties (error bars represent ± 1 s.d.).

Finding 2: fragment-partner spins uncorrelated

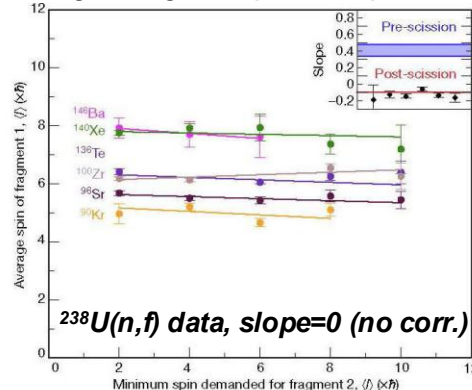


Fig. 2 | Correlation between fragment spins. Correlations between fragment and partner spins for the six most strongly populated fragments in the $^{238}\text{U}(n, f)$ reaction with associated statistical uncertainties (error bars represent ± 1 s.d.). Weighted linear fits to the data points for each nucleus are shown. The fitted slopes are compared to the expected slopes for the spin mechanisms pre-scission with correlated spins ('Pre-scission') or post-scission with uncorrelated spins ('Post-scission') in the Inset. The blue band ('Pre-scission') was determined from Monte-Carlo simulations of the de-correlating effects of the neutrons and statistically-rare

Conclusion:

Finding 2 corresponds to one of the authors' expectations and seems to suggest: angular-momentum generation happens "post-scission"

Experimental

γ -ray multiplicities for 3 data sets

ALTO facility Orsay

- neutron source
- v-Ball γ -ray array

^{252}Cf set taken w/ additional IC

Equilibrium statistical treatment of angular momenta associated with collective modes in fission and heavy-ion reactions

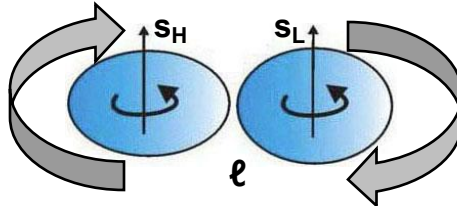
Luciano G. Moretto and Richard P. Schmitt

Lawrence Berkeley Laboratory, University of California, Berkeley, California 94720
(Received 14 May 1979)

The angular momentum effects in deep inelastic processes and fission have been studied in the limit of statistical equilibrium. The model consists of two touching liquid drop spheres. Angular momentum fractionation has been found to occur along the mass asymmetry coordinate. If neutron competition is included (i.e., in compound nucleus formation and fission), the fractionation occurs only to a slight degree, while extensive fractionation is predicted if no neutron competition occurs (i.e., in "fusion-fission" without compound nucleus formation). Thermal fluctuations in the angular momentum are predicted to occur due to degrees of freedom which can bear angular momentum such as wriggling, tilting, bending, and twisting. The coupling of relative motion to one of the wriggling modes, leading to fluctuations between orbital and intrinsic angular momentum, is considered first. Next the effect of the excitation of all the collective modes on the fragment spin is treated. General expressions for the first and second moments of the fragment spins are derived as a function of total angular momentum and the limiting behavior at large and small total angular momentum is examined. Furthermore, the effect of collective mode excitation on the fragment spin alignment is explored and is discussed in light of recent experiments. The relevance of the present study to the measured first and second moments of the γ -ray multiplicities as well as to sequential fission angular distributions is illustrated by applying the results of the theory to a well studied heavy-ion reaction.

Angular momentum conservation

Wriggling: $s_H + s_L + \ell = s_0 = 0$ (^{252}Cf)



Bending & Twisting: pairwise cancellation of fragment spins

Tilting: similar to wriggling

AM projection onto fission axis: $K=0$ (W&B), $K>0$ (T&T)

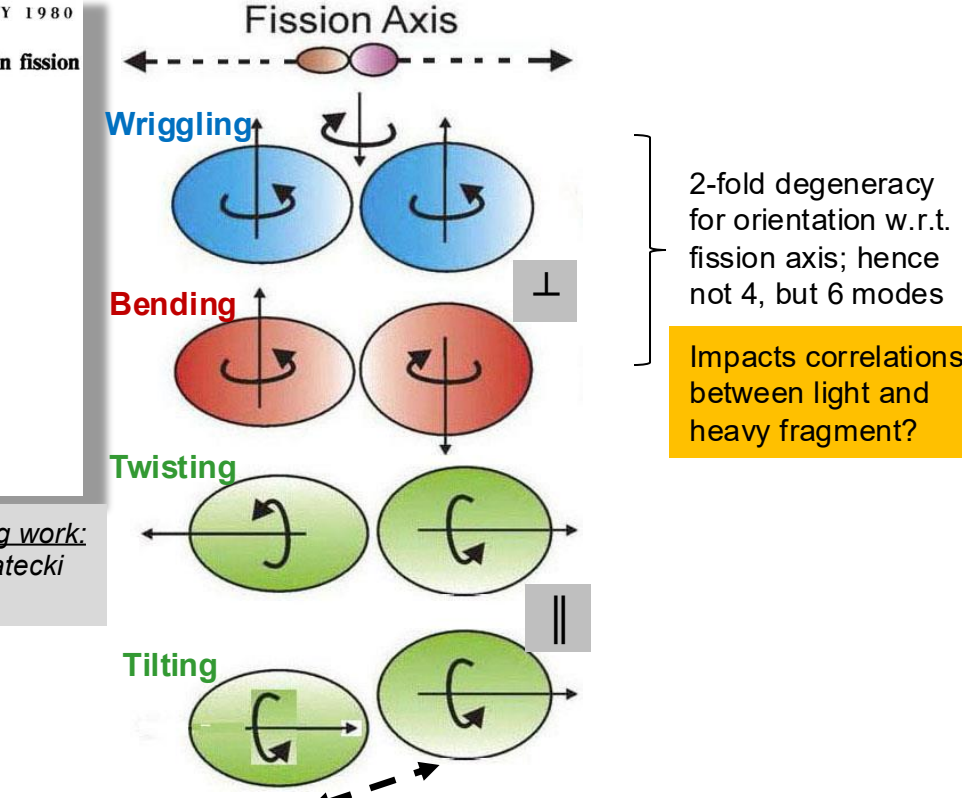


Illustration: J. Snyder, PhD Thesis
W.U. St. Louis (2014)

Generation of Fragment Angular Momentum in Fission

Jørgen Randrup¹ and Ramona Vogt^{2,3}¹Nuclear Science Division, Lawrence Berkeley National Laboratory, Berkeley, California 94720, USA²Nuclear & Chemical Sciences Division, Lawrence Livermore National Laboratory, Livermore, California 94551, USA³Physics and Astronomy Department, University of California, Davis, California 95616, USA

(Received 19 March 2021; revised 23 April 2021; accepted 16 June 2021; published 5 August 2021)

A recent analysis of experimental data [J. Wilson *et al.*, *Nature (London)* **590**, 566 (2021)] found that the angular momenta of nuclear fission fragments are uncorrelated. Based on this finding, the authors concluded that the spins are therefore determined only *after* scission has occurred. We show here that the nucleon-exchange mechanism, as implemented in the well-established event-by-event fission model FREYA, while agitating collective rotational modes in which the two spins are highly correlated, nevertheless leads to fragment spins that are largely uncorrelated. This counterexample invalidates the conclusion in [J. Wilson *et al.*] that uncorrelated spins must necessarily have been generated after scission

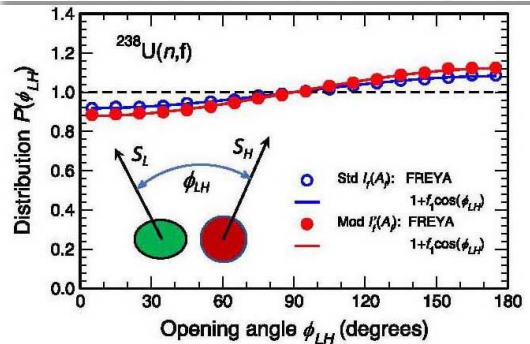


FIG. 1. The distribution of the opening angle ϕ_{LH} between the angular momenta of the two fission fragments from $^{238}\text{U}(n, f)$, as obtained by FREYA using either the standard moment of inertia, $I_f(A_f) = 0.5I_{\text{rig}}(A_f)$ (dots) or the modified form depending on the shapes of the fragments at scission, $I'_f(A_f)$ (open circles). Also shown are the corresponding lowest-order Fourier approximations, $P(\phi_{LH}) = 1 + f_1 \cos \phi_{LH}$.

FREYA code

Effect of 2-fold degeneracy...

NB: spin generated “pre-scission” (model)

Many rolls of the dice:

The red & blue dice are cast for many rounds: Alice's score is the sum of the top faces; Bob's score is the sum of the top of the red dice and the bottom of the blue dice

Alice:



Bob:



same as Alice opposite of Alice *i.e. 2-fold degen.*

Alice	Bob
6 + 5 = 11	6 + 2 = 8
2 + 1 = 3	2 + 6 = 8
1 + 5 = 6	1 + 2 = 3
3 + 3 = 6	3 + 4 = 7
5 + 4 = 9	5 + 3 = 8
2 + 4 = 6	2 + 3 = 5
3 + 5 = 8	3 + 2 = 5
5 + 3 = 8	5 + 4 = 7
1 + 4 = 5	1 + 3 = 4
2 + 1 = 3	2 + 6 = 8
....

In each round, the score contributions for Bob are fully correlated with the corresponding score contributions for Alice

Nevertheless, Bob's scores are uncorrelated with Alice's scores

The two score sequences are
not correlated

Slide: R. Vogt, communicated through L. Sobotka

Preliminary summary of data vs. theory controversy

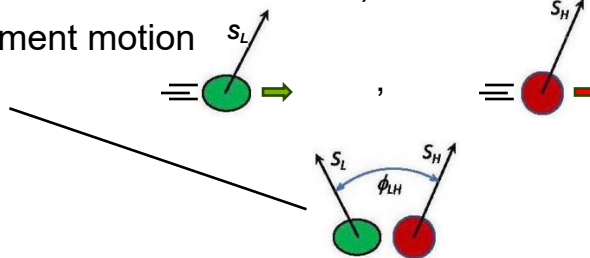
Wrapping it up...

Wilson et al. showed experimental evidence for uncorrelated fission-fragment-spin magnitude. Randrup and Vogt don't question the observation, they object to the logic that spin generation happens "post-scission" (lack of correlations is an a-priory expectation of the R&V model).

Objectives

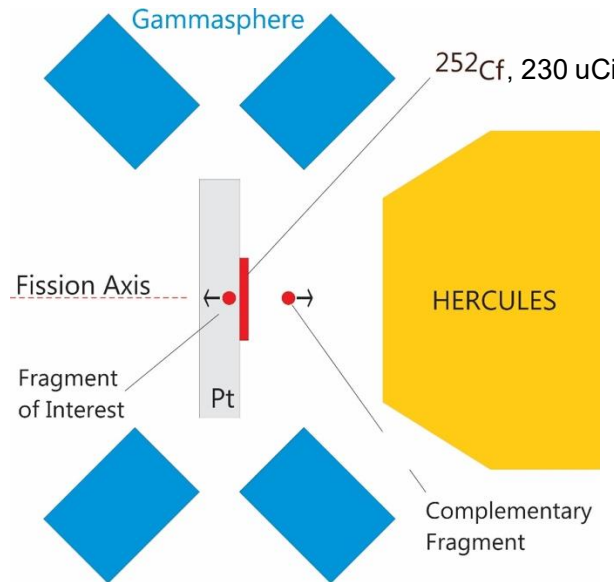
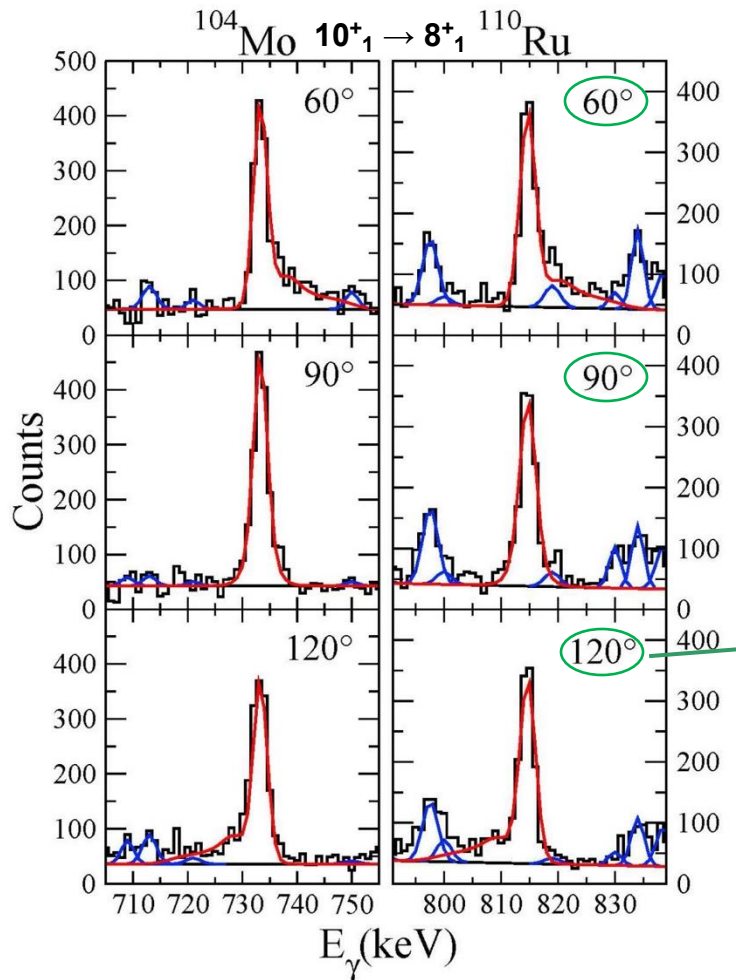
γ -ray angular-distributions and -correlations (between fiss. fragmets) can shed light on the issues.

- 1) Orientation of the fragment spins w.r.t. fragment motion
- 2) Relative orientation of the fragment spins!
- 3) Magnitudes of the intrinsic spins?

Approach (as a starter)

- 1) Practice spectroscopy especially angular-distribution analysis w/ fission axis as orientation axis; this feature is absent in Wilson et al. despite that an IC was used
- 2a) Consider using two γ lines where one is a Doppler shifted and the other one a stopped peak; this implies having a fission fragment detected (next slide)
- 2b) Develop a method of "inter" correlations between LF and HF; rather than analyzing "intra"

correlations for either one fragment



Angle: \star Fission Axis, γ -ray detector

Measure fragment velocity as well

Two types γ 's: "partially/fully stopped", Doppler shifted

Gating by LF or HF; no β -decay γ 's

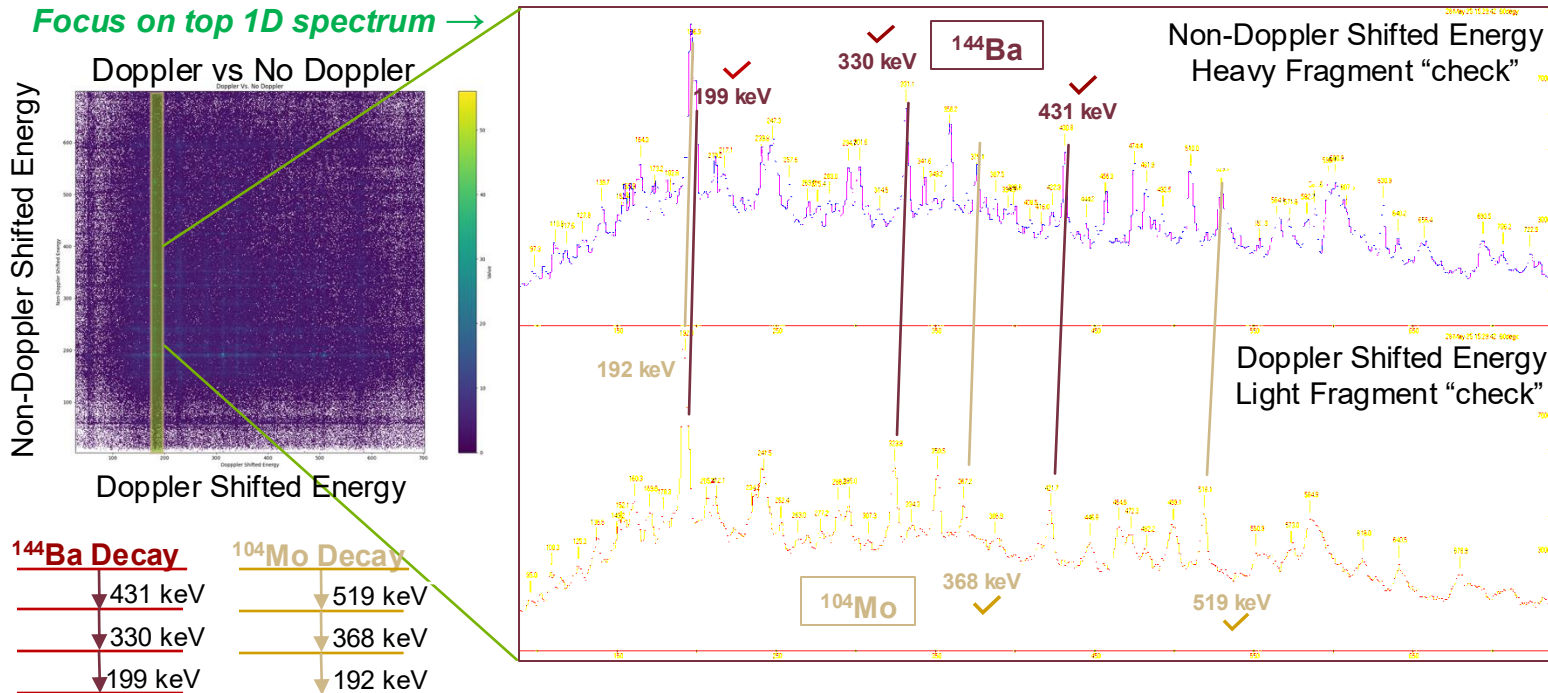
Stat's: $2.1 \cdot 10^9$ fragment- γ^4 quintuples

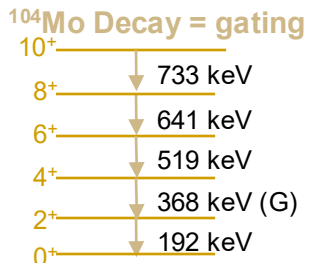
Additional comments

Q_t measurements for $^{102-108}\text{Mo}$, $^{108-112}\text{Ru}$; evidence for a triaxial shape at medium to high spin.

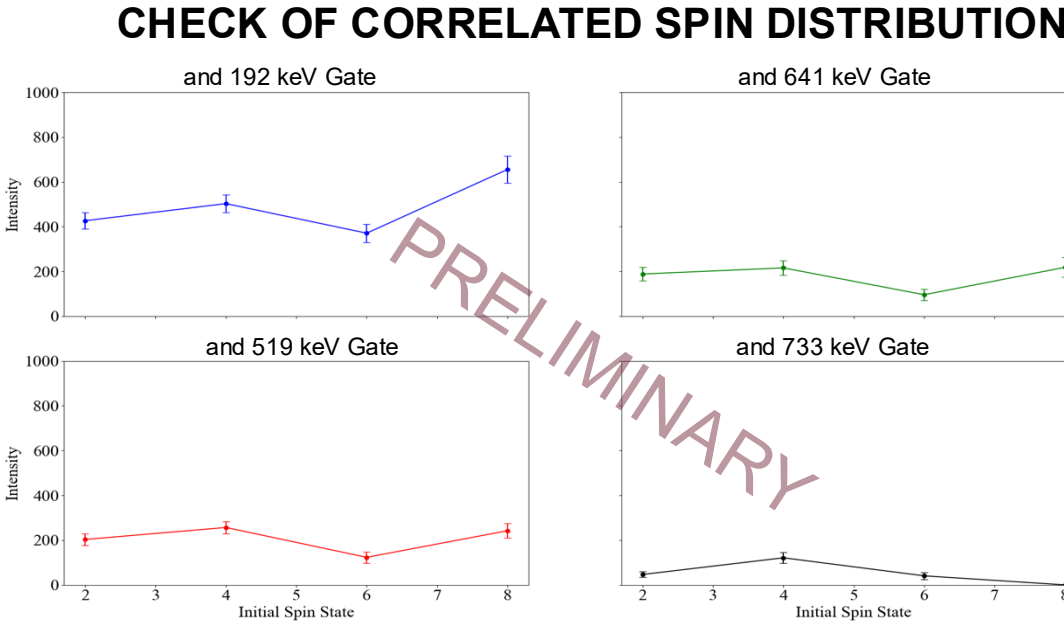
Motivation for the development of the UNEDF0 energy density functional by Zhang, Bhatt, and Nazarewicz.

CORRELATIONS THROUGH DOPPLER SHIFTING





- Requiring coincident γ 's for ¹⁰⁴Mo (require 368 keV and corresponding label)
- Plotting efficiency corrected ¹⁴⁴Ba γ intensities



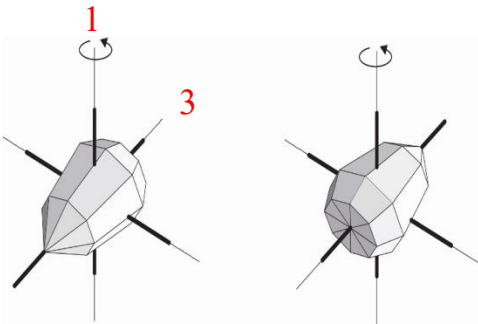
¹⁴⁴Ba γ intensity with two coincident ¹⁰⁴Mo gates

→ Similar intensity patterns regardless of gate applied – the spin of LF has no correlation w/ the spin of HF

Not only that this result is expected, but this type of analysis isn't the prime objective of the present analysis.

Heading now towards LF, HF γ -angular correlation analysis.

REFLECTION-ASYMMETRIC NUCLEAR SHAPE ($\beta_3 \neq 0$)



$R = \exp(-i\pi I)$	Half-turn around axis 1	No
X	Mirror symmetry w.r.t. a plane containing axis 1 and not axis 3	No
$S = PR^{-1}$	Mirror symmetry w.r.t. a plane containing axes 1 and 3 (P:parity)	Yes

“combined q.n.”
(B/M Vol. II)

Spin selection rules: half-integer spin

$$S = P \exp(i\pi I) = P \cos(\pi I) + P i \sin(\pi I)$$

$$S = -i \quad I^P = 1/2^-, 5/2^-, 9/2^-, \dots \text{ and } 3/2^+, 7/2^+, 11/2^+, \dots$$

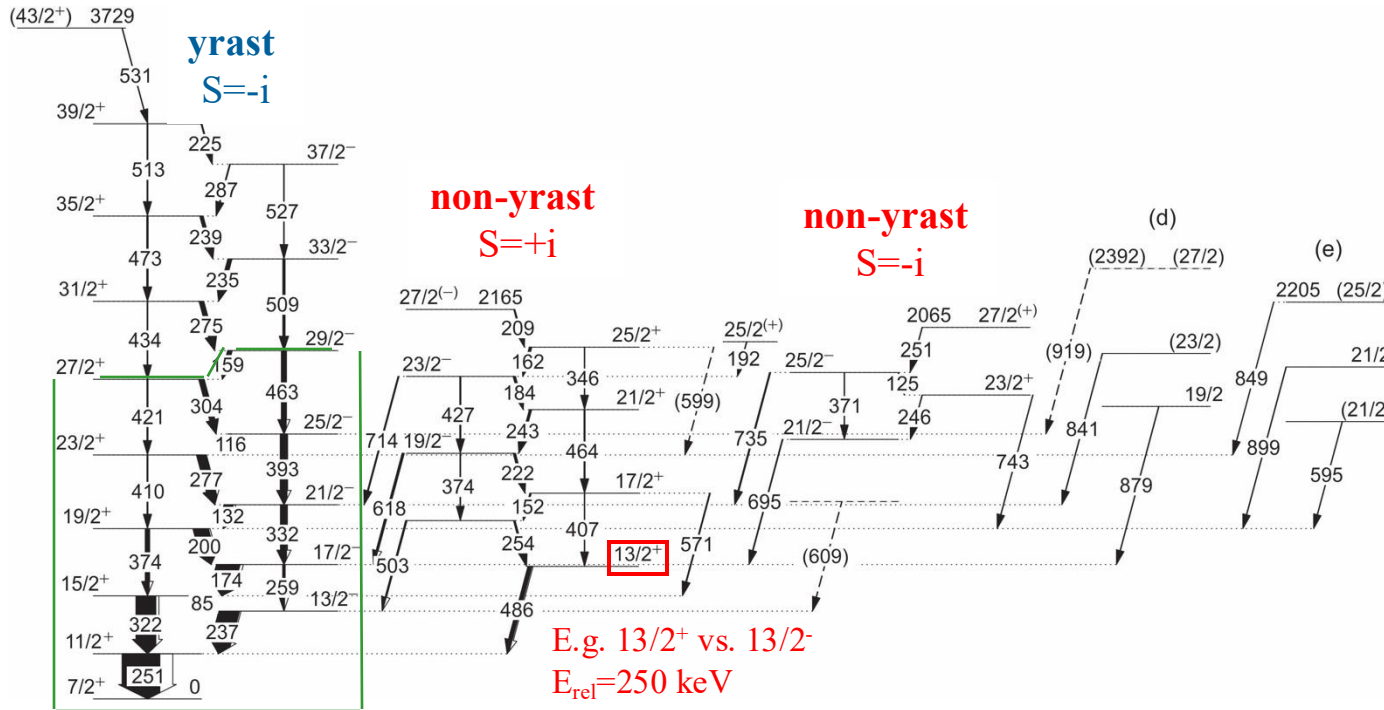
$$S = +i \quad I^P = 1/2^+, 5/2^+, 9/2^+, \dots \text{ and } 3/2^-, 7/2^-, 11/2^-, \dots$$

The simplex fixes the spin for a given parity!

NB both $S = -i$ and i have been observed often.

For integer spin: $S = 1$ and -1 ; the latter has been only observed for non-yrast sequences.

Additional comment: Octupole correlations provide a good example how the symmetry of the mean field dictates the spin-parity sequence of the level structure irrespective the degree of deformation and or the configuration. The “zigzag” pattern is present in different band structures and over a large spin range.



Previous work: Dahlinger et al. NPA 484 (1988)

Intensity difference:
about factor of 5

Reviol et al., PRC 90, 044318 (2014) [GSFMA202]

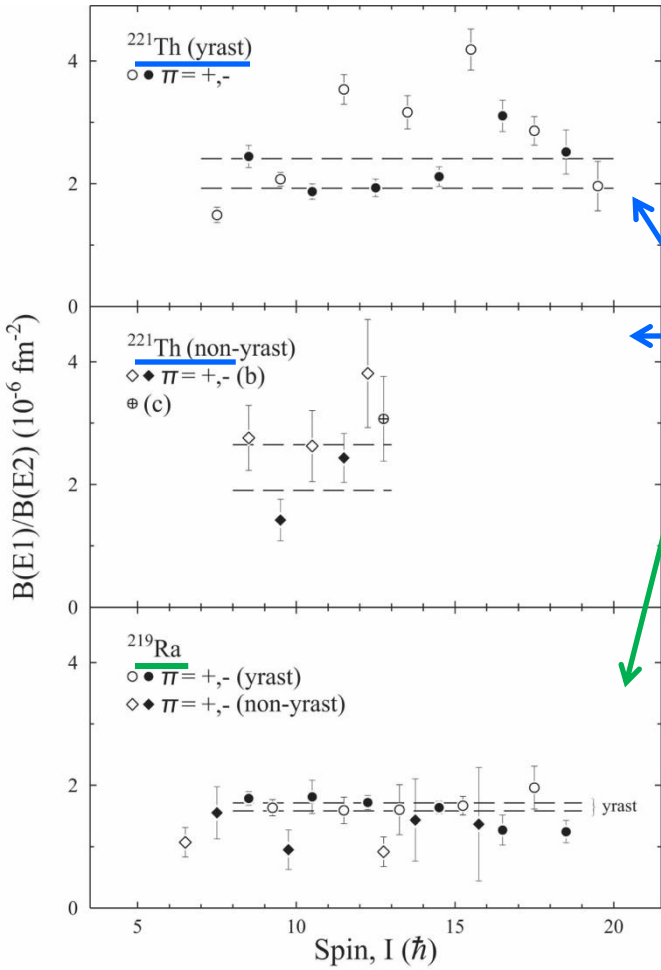
Comments

Yrast vs. non-yrast:
1 vs. 2 degenerated
simplex bands;

Assignments: K=1/2 for yrast, K=5/2 for non-yrast band (same as ^{223}Th , yrast);

Basis for assignments:
B(E1)/B(E2) info - see
next slide - as well as
deduced B(M1) values,

Studying the present scenario has clarified: for octup. sequences with $K \geq 3/2$ degenerate parity doublets can be expected;



B(E1)/B(E2) Information

Nucleus	$B(E1)/B(E2)$ (10^{-6} fm^{-2})	expt.		theory		
		$\langle \beta_3 \rangle$	$2\beta_3$	β_3	β_2	K
$^{221}\text{Th (y)}$	2.17 (24)	0.215 (12)	0.180	0.090	0.101	$1/2$
$^{221}\text{Th (n-y)}$	2.28 (37)	0.220 (18)	0.220	0.110	0.094	$5/2$
^{221}Th				0.083	0.096	$3/2^+$
^{223}Th	1.68 (32)	0.189 (18)	0.212	0.106	0.118	$5/2$
^{225}Th	0.83 (31)	0.133 (25)	0.216	0.108	0.137	$3/2$
$^{219}\text{Ra (y)}$	1.65 (7)	0.188 (4)	0.166	0.083	0.092	$1/2$
$^{219}\text{Ra (n-y)}$	1.07 (28)	0.151 (19)	0.142	0.071	0.088	$3/2$
^{219}Ra				0.106	0.084	$5/2^+$
^{221}Ra	0.93 (14)	0.141 (10)	0.202	0.101	0.107	$5/2$

^aEnergetically less favorable according to theory

$$B(E1)/B(E2) \approx 2.694 \cdot c_{ld}^2 \cdot A^{2/3} \cdot \langle \beta_3^2 \rangle \text{ fm}^{-4}$$

$$c_{ld} = 6.9 \cdot 10^{-4} \text{ fm} ; \beta_3 = \text{const.}$$

Assignments are confirmed by B(M1) data.

Ref.: Reviol et al., PRC 90, 044318 (2014) [expt.]
 Cwiok & Nazarewicz, NPA 529, 95 ('91) [table]
 Nazarewicz & Olanders, NPA 441, 420 ('85) [c_{ld}]

Additional comments

This provided evidence for configuration dependent differences in β_3 (on a relative scale though).

The factor 2 adjustment means: D_0 calculated in liquid-drop style is underpredicted by the same factor.

Until very recently, this has been the only such B(E1)/B(E2) comparison of experiment vs. theory.

That comparison, for ^{120}Ba , uses RHB density functional theory, but D_0 is overpredicted [Lv et al. (2022)].

Nuclear physics ingredients of EDM measurements

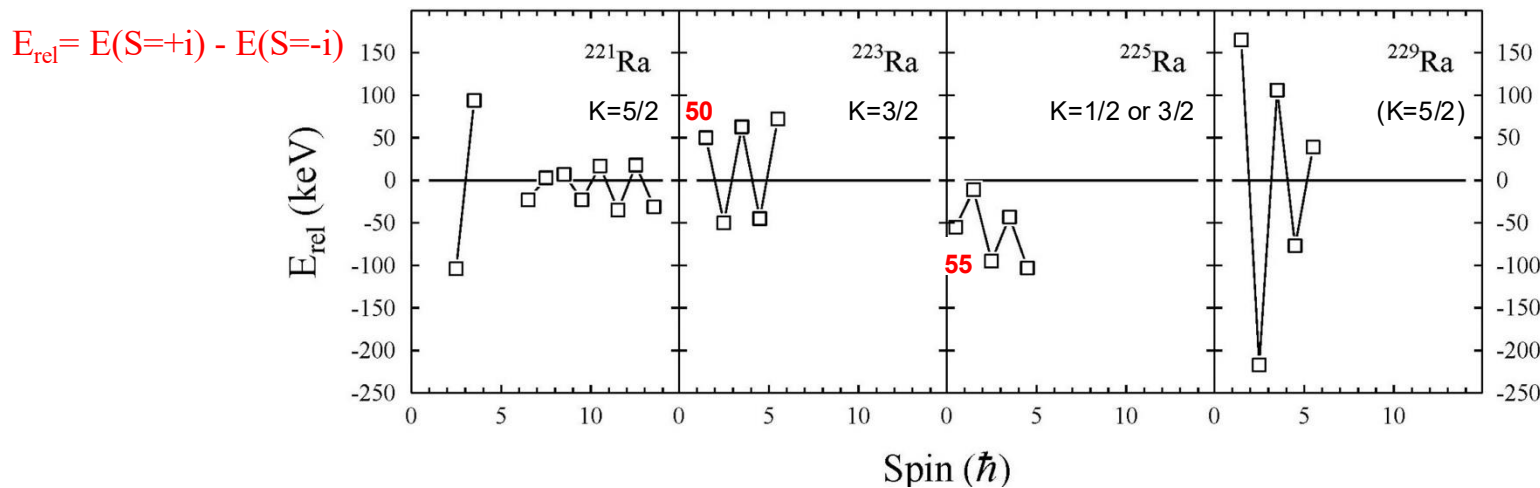
In a nutshell...

Objective: Atoms should get an EDM from their nucleus; but is it measurable?

Selecting an odd-A nucleus: It is said that a near degenerate parity doublet introduces parity violating terms in the Hamiltonian; *Haxton & Henley PRL 51, 1937 (1983)*

Optimization: β_3 large \uparrow , $E_{\text{rel}, \text{P-doublet}}$ small \downarrow , Z large \uparrow

Example: Ra nuclei near ^{226}Ra are “long lived” (10d) and available at “large” quantities (750 ng, $2 \cdot 10^{15}$ atoms)



Given that there is a high demand for $^{223,225}\text{Ra}$ (e.g. for Ra-molecule based RDM experiments) RVFJ, ADA, et al. have a Coulex project to study ^{223}Ra : E3 m.e. [$B(E3\downarrow)$: 30-60 W.u.], level scheme confirmation.

Thank you for your attention!

Congratulations, Robert!



BACKUP SLIDES

Spatial orientation of the fission fragment intrinsic spins and their correlations

Guillaume Scamps¹, Ibrahim Abdurrahman², Matthew Kafker,¹ Aurel Bulgac¹, and Ionel Stetcu^{1,2}¹Department of Physics, University of Washington, Seattle, Washington 98195-1560, USA²Theoretical Division, Los Alamos National Laboratory, Los Alamos, New Mexico 87545, USA

(Received 26 July 2023; revised 22 September 2023; accepted 21 November 2023; published 26 December 2023)

New experimental and theoretical results obtained in 2021 made it acutely clear that more than 80 years after the discovery of nuclear fission we do not understand the generation and dynamics of fission fragment (FF) intrinsic spins well, in particular their magnitudes, their spatial orientation, and their correlations. The magnitude and orientation of the primary FFs have a crucial role in defining the angular distribution and correlation between the emitted prompt neutrons, and subsequent emission of statistical (predominantly $E1$) and stretched $E2$ γ rays, and their correlations with the final fission fragments. Here, we present detailed microscopic evaluations of the FF intrinsic spins, for both even- and odd-mass FFs, and of their spatial correlations. These point to a well-defined three-dimensional FF intrinsic spin dynamics, characteristics absent in semiphenomenological studies, due to the presence of the twisting spin modes, which artificially were suppressed in semiphenomenological studies.

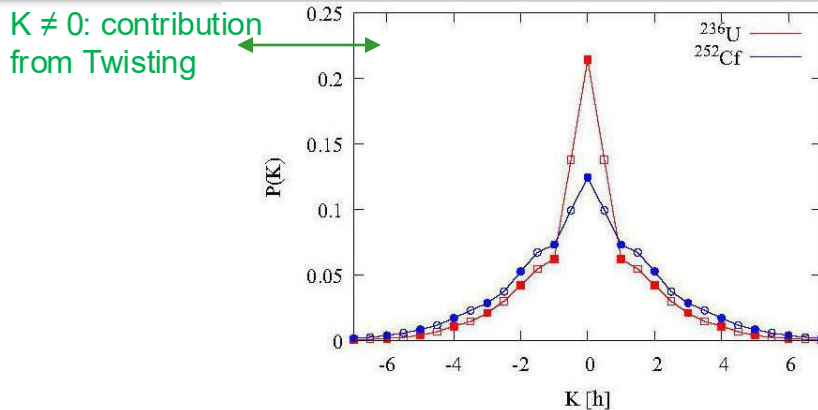


FIG. 2. Top: The distribution of the K quantum number. Since $K_H + K_L = 0$ the distributions for heavy and light FFs are identical. The integer K values are shown with filled symbols and with empty symbols for half-integer K values.

Theory – theory controversy

In a nutshell...

Semi-phenomenological approach

$K \neq 0$ modes frozen (due to \Im considerations), “2D” picture;
FREYA code of Randrup et al.

Time-dependent DFT theory

$K \neq 0$ modes permitted, “3D”;
Bulgac, Scamps et al.

Accepted by both groups: validity of 6 collective modes (“pre-fission”)

Angular distributions of specific gamma rays emitted in the deexcitation of prompt fission products of $^{252}\text{Cf}^\dagger$

A. Wolf* and E. Cheifetz

Department of Nuclear Physics, Weizmann Institute of Science, Rehovot, Israel

(Received 5 February 1976)

Angular distributions of specific γ rays emitted in the deexcitation of prompt fission products of ^{252}Cf were measured with respect to the fission direction. A total of 42 angular distributions were measured, 23 of which were transitions in even-even fragments.

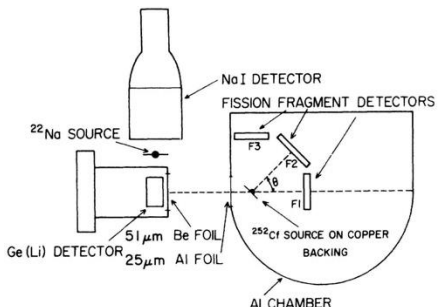


FIG. 1. Schematic description of the experimental setup. Relative distances and sizes of detectors are shown to scale.

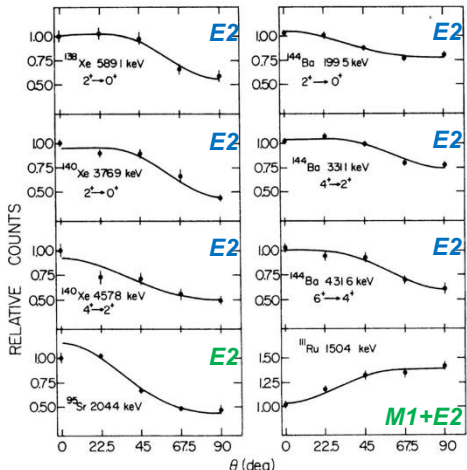


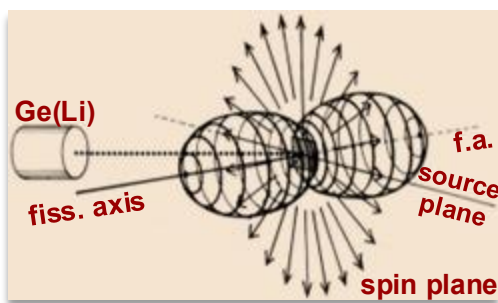
FIG. 3. Angular distributions of several transitions measured in this work. The solid lines were obtained by a least-squares-fitting procedure to $W(\theta) = a_0[1 + A_2 P_2(\cos \theta) + A_4 P_4(\cos \theta)]$.

Data: γ -fragment correlated events

even-even and odd-A nuclei

Result ($^{138,140}\text{Xe}$, $^{142,144}\text{Ba}$):

angular momentum must be oriented in a plane perpendicular to fission axis



Theoretical study of triaxial shapes of neutron-rich Mo and Ru nuclei

C. L. Zhang (张春莉),^{1,2} G. H. Bhat,³ W. Nazarewicz,^{1,4,5} J. A. Sheikh,³ and Yue Shi (石跃)¹

¹Department of Physics and Astronomy and NSCL/FRIB Laboratory, Michigan State University, East Lansing, Michigan 48824, USA

²State Key Laboratory of Nuclear Physics and Technology, School of Physics, Peking University, Beijing 100871, China

³Department of Physics, University of Kashmir, Srinagar, 190 006, India

⁴Physics Division, Oak Ridge National Laboratory, Oak Ridge, Tennessee 37831-6373, USA

⁵Institute of Theoretical Physics, Faculty of Physics, University of Warsaw, Pasteura 5, PL-02-093 Warsaw, Poland

(Received 16 July 2015; published 10 September 2015)

Background: Whether atomic nuclei can possess triaxial shapes at their ground states is still a subject of ongoing debate. According to theory, good prospects for low-spin triaxiality are in the neutron-rich Mo-Ru region. Recently, transition quadrupole moments in rotational bands of even-mass neutron-rich isotopes of molybdenum and ruthenium nuclei have been measured. The new data have provided a challenge for theoretical descriptions invoking stable triaxial deformations.

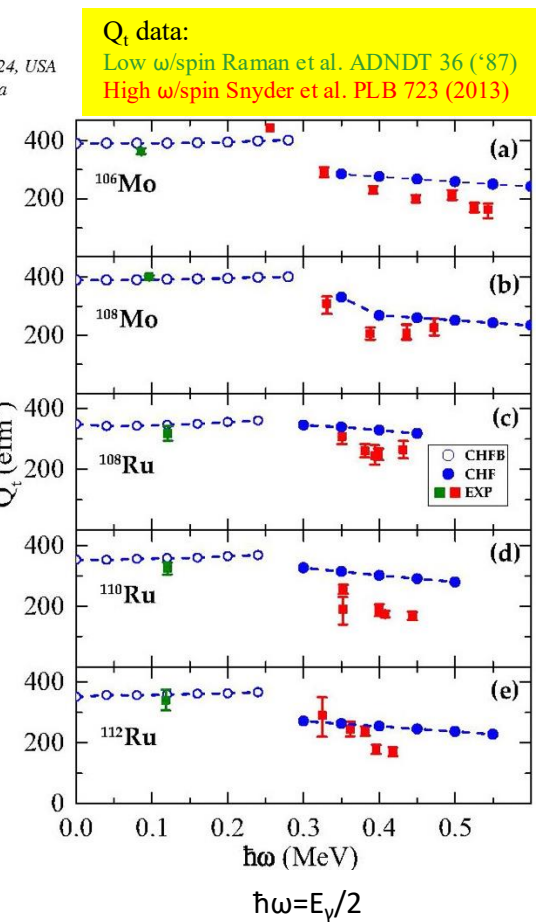
Purpose: To understand experimental data on rotational bands in the neutron-rich Mo-Ru region, we carried out theoretical analysis of moments of inertia, shapes, and transition quadrupole moments of neutron-rich even-even nuclei around ^{110}Ru using self-consistent mean-field and shell model techniques.

Methods: To describe yrast structures in Mo and Ru isotopes, we use nuclear density functional theory (DFT) with the optimized energy density functional UNEDF0. We also apply triaxial projected shell model (TPSM) to describe yrast and positive-parity, near-yrast band structures.

Results: Our self-consistent DFT calculations predict triaxial ground-state deformations in $^{106,108}\text{Mo}$ and $^{108,110,112}\text{Ru}$ and reproduce the observed low-frequency behavior of moments of inertia. As the rotational frequency increases, a negative- γ structure, associated with the aligned $(h_{11/2})^2$ pair, becomes energetically favored. The computed transition quadrupole moments vary with angular momentum, which reflects deformation changes with rotation; those variations are consistent with experiment. The TPSM calculations explain the observed band structures assuming stable triaxial shapes.

Conclusions: The structure of neutron-rich even-even nuclei around ^{110}Ru is consistent with triaxial shape deformations. Our DFT and TPSM frameworks provide a consistent and complementary description of experimental data.

FIG. 9. (Color online) Transition quadrupole moments for $^{106,108}\text{Mo}$ and $^{108,110,112}\text{Ru}$ calculated in CHFB (open circles) and CHF (dots) compared to experiment.

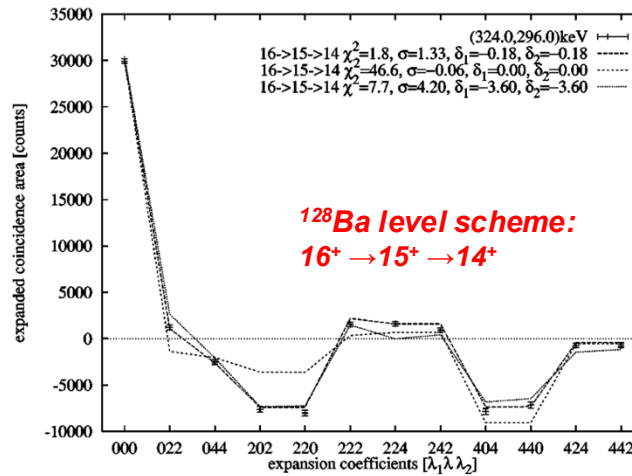


Testing UNEDF0 energy density functional

METHOD FOR γ ANGULAR CORRELATION

Spectral Expansion of DCO – SpeeDCO

- Good for large numbers of geometric correlations; like Gammasphere
- DCO distributions form a complete orthogonal basis
- Perform analysis on coincident gammas in that basis
- Shown to be a valid way to determine spins and multipolarity-mixing ratios (δ) of states in ^{128}Ba



Wiedenhöver et al. PRC 58, 721 (1998)

SpeeDCO for fission – present thoughts

- Method allows for the event-by-event transformation of data; increment several float-point matrices with the value of the corresponding Legendre polynomial (could be negative, no sweat).
- Applying the correct γ gates, we should be able to determine angular correlation between γ 's of fission fragments.

219Th₁₂₉

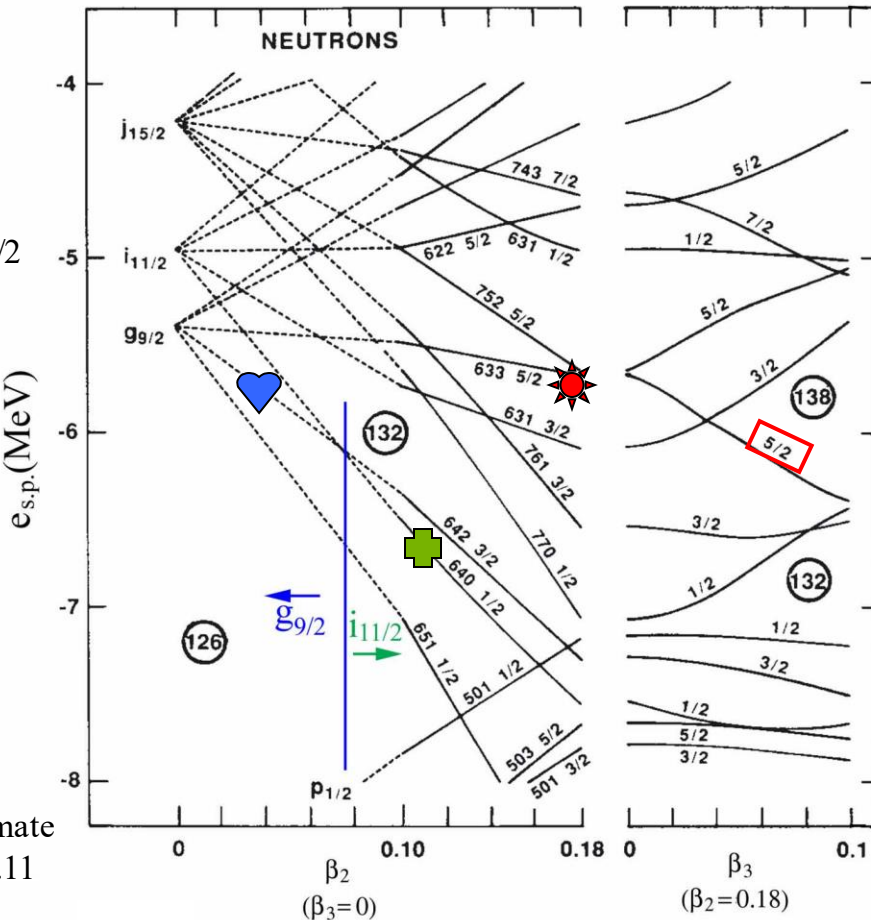
$$(g_{9/2})^3 \text{ K}=3/2$$

221Th₁₃₁

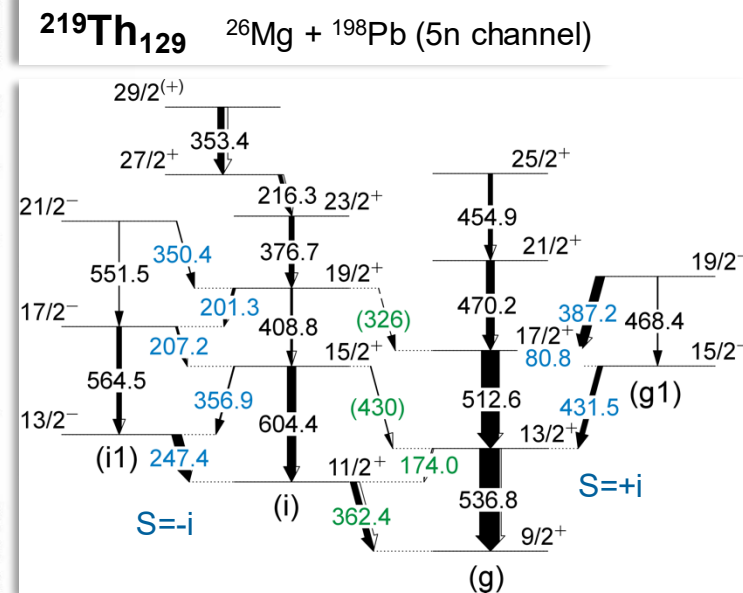
$$i_{11/2}(g_{9/2})^4 \text{ K=1/2}$$

223Th₁₃₃

$$(i_{11/2})^2(g_{9/2})^5$$



Grodzins estimate
for ^{221}Th : $\beta_2 = .11$

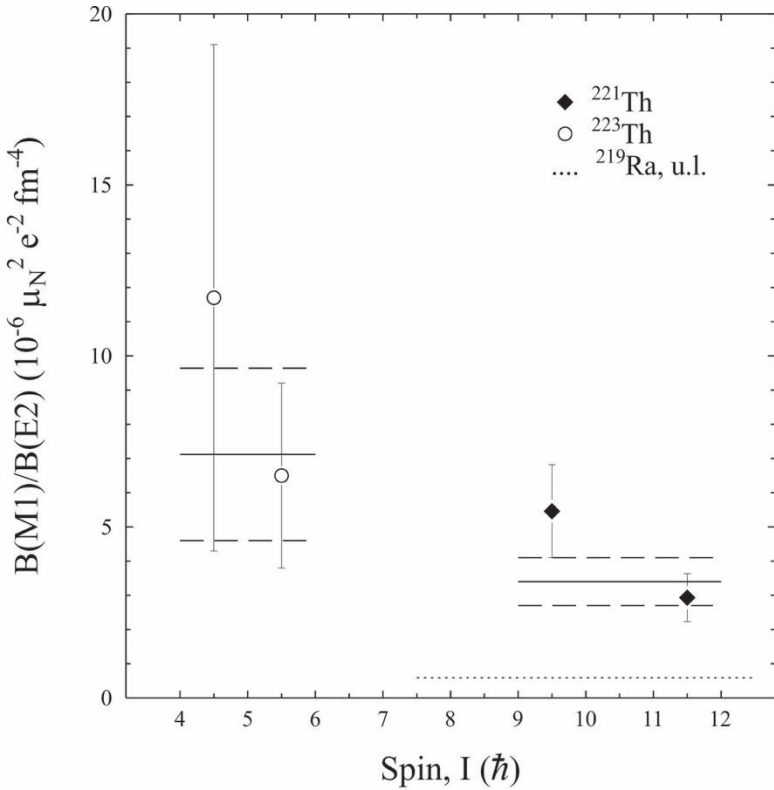


E.g. $13/2^+$ vs. $13/2^-$: $E_{\text{rel}} = -80$ keV

$$B(E1)/B(E2)_{avg} = 1.26(81) \text{ fm}^{-2}$$

Reviol et al., PRC 80, 011304R (2009) [GSFMA154]

B(M1)/B(E2) analysis



Nucleus (Ref.)	$B(M1)_{\text{avg}}$ [$10^{-2} \mu_N^2$]	$K^a)$
^{220}Th (Reviol '14)	0.29 (3)	0.07
^{226}Th (Dahlinger '88)	0.30 (1)	0.21
^{228}Th (Wieland '92) ^{b)}	0.12 (3)	0.11

a) Suggested K

b) Wieland et al., PRC 45, 1035 ('92)

B(E2) from Grodzins estimate

Survey of $3^- \rightarrow 0^+$ B(E3) data

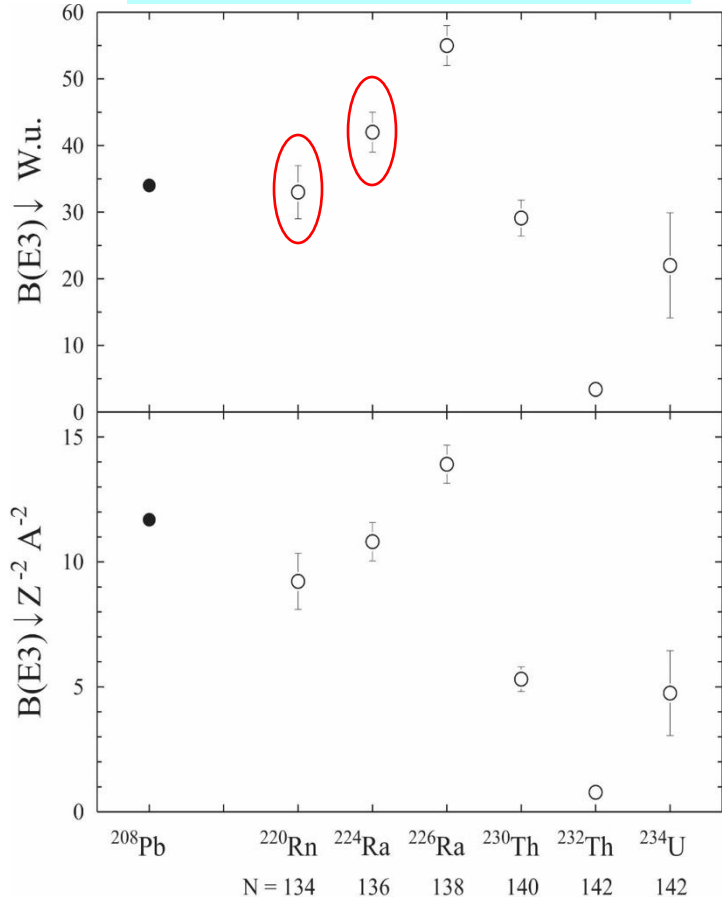
Ref:
Spear,
ADNDT 42 (1989)

Gaffney et al.,
Nature 497 ('13)

Wollersheim et al.,
NPA 556 (1993)

$$B(E\lambda) \propto Q_\lambda^2$$

$$Q_\lambda \propto Z \cdot A^{\lambda/3} \cdot \beta_\lambda$$



Recent RIB measurements

The $N = 134 - 138$ data points are elevated w.r.t. the heavier, higher- N cases.

This is in line with the location of the lowest $\pi = -$ states ($N = 134, 136$).